Seismicity in Central Oklahoma shows features of reservoir-induced seismicity

L. Johann, S. A. Shapiro & C. Dinske

Freie Universität Berlin, Institute of Geophysics

7 March, 2019

www.nature.com/scientificreports

SCIENTIFIC REPORTS

OPEN

The surge of earthquakes in Central Oklahoma has features of reservoir-induced seismicity

Received: 9 April 2018

Accepted: 19 July 2018

Published online: 31 July 2018

Lisa Johann, Serge A. Shapiro & Carsten Dinske

The recent surge of seismicity in Oklahoma and Kansas is related to fluid disposal. Evidences suggest that critical parameters are the injection volume as well as injection depth but dominant physical processes and a corresponding model to describe the physics are still not clear. We analyse the spatio-temporal distribution of induced earthquakes in the basement and find visible signatures of pore pressure diffusion and poroelastic coupling, features which strongly resemble seismicity induced by the filling of artificial lakes, so-called reservoir-induced seismicity. We developed a first-principle model of underground reservoir-induced seismicity. The physics of the model are based upon the combined mechanisms of fluid mass added to the pore-space of the injection layer and acting as a normal stress on the basement surface, pore-fluid pressure diffusion in the basement as well as poroelastic coupling contributing to the pore-fluid pressure and stress. Furthermore, we demonstrate that underground reservoir-induced seismicity occurs preferably in normal faulting and strike-slip settings, the latter being prevalent in Oklahoma. Our model explains observed injection volume and depth dependence of the seismicity and should be considered as a basis for future hazard prediction and prevention as well as for planning possible disposal sites.

Starting in 2009, an unexpected burst of earthquakes has struck the central U.S.[1,2]. Whereas only about one magnitude $M \geq 3$ earthquake happened per year in north-central Oklahoma before 2009, approximately 900 $M \geq 3$ events were recorded in 2015[3]. It is now widely understood that this acceleration of seismic activity is linked to the injection of huge volumes of waste water through salt water disposal (SWD) wells[2,3]. Most of these wells inject into the highly permeable, underpressured Arbuckle aquifer which is hydraulically connected to the underlying crystalline basement where most of the seismicity occurs. In reaction to the strong increase of earthquakes, the Oklahoma Corporation Commission (OCC) Oil and Gas Division called for a 40% reduction of the 2014 injection volume in Central Oklahoma to be completed in mid- 2016.

Numerous studies on mechanisms explaining the spatio-temporal evolution of the observed fluid-disposal induced seismicity have been published to date. There are indications that the injection volume as well as injection depth affect the seismic activity[4]. However, it remains a challenging task to assess the governing physical processes because they are assumed to deviate from the ones which control seismicity induced by high-pressure reservoir stimulations[5,6]. For the case of Oklahoma, firstly, events occur in the deeper basement and not directly in the overlying injection formation. Secondly, seismicity is also observed over broad areas far from injectors. And thirdly, unlike in the case of pure pore-fluid pressure diffusion where the spatio-temporal event evolution is enveloped by a triggering front[7], the time and location of earthquakes in Oklahoma does not clearly obey such a

Johann et al. (2018)

Motivation

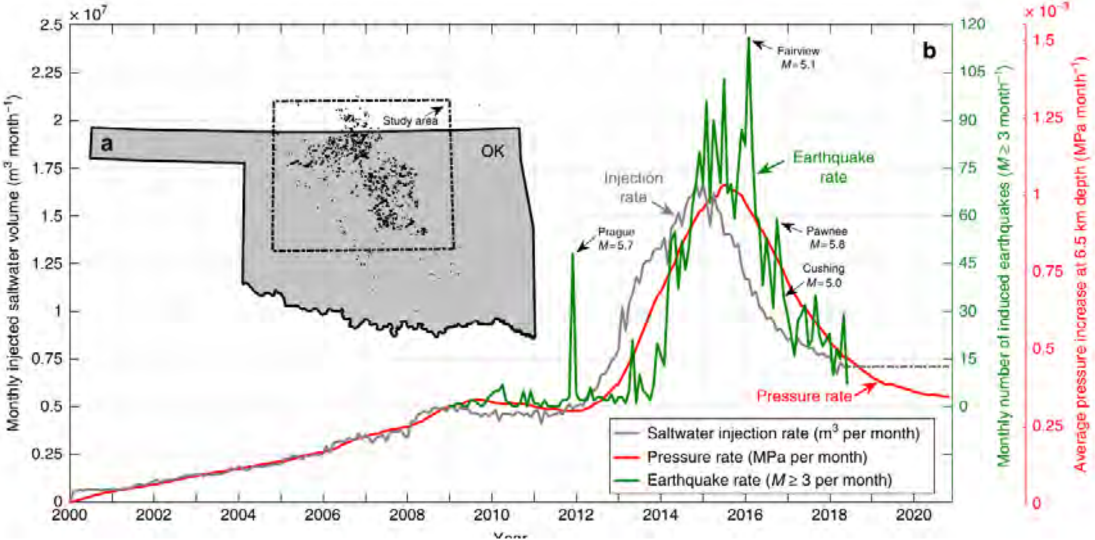

(From Langenbruch et al., 2018)

- seismicity at 2 - 5 km below top of the basement (TOB) $\rightarrow$ aseismic gap below TOB
- numerous injectors $\rightarrow$ cumulative volume effect
- events occur occasionally far from single high-volume injectors

$\Rightarrow$ **Can we derive a model explaining these features?**

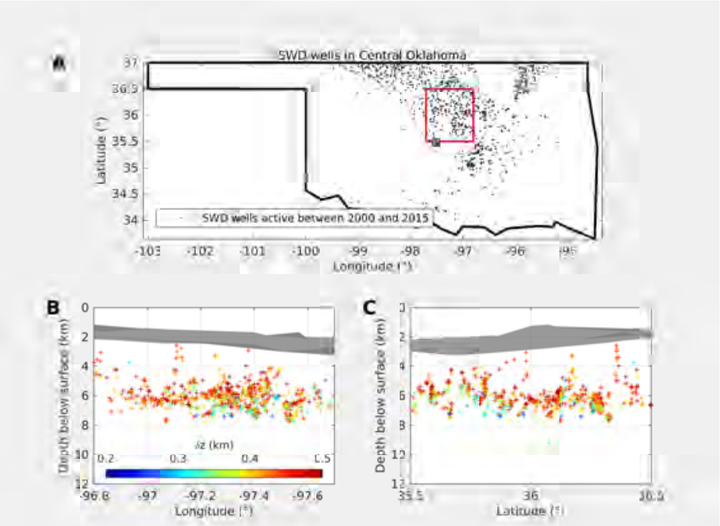

(Catalog from Schoenball and Ellsworth, 2017)

Reservoir-Induced Seismicity

see e.g. Talwani (1997), Simpson et al. (1988)

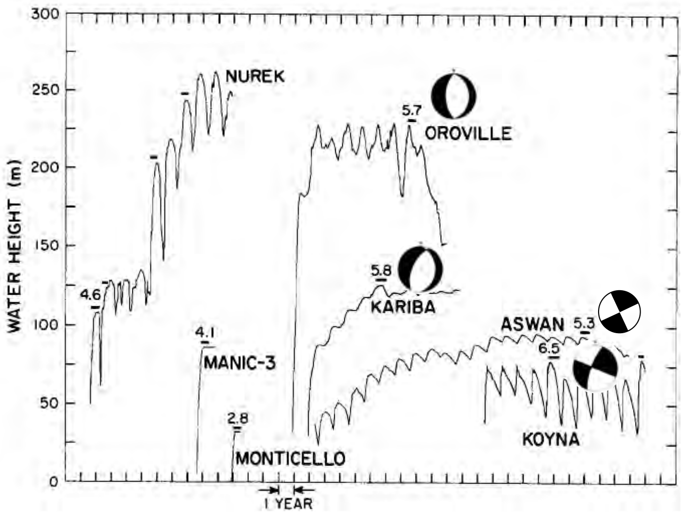

(Modified after Simpson et al., 1988)

Conceptual Model: Underground Reservoir-Induced Seismicity

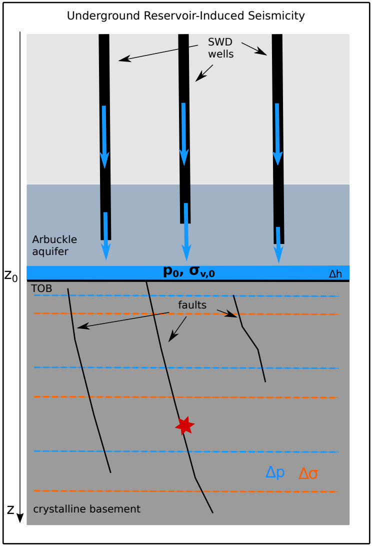

Note:

p_0: pore-fluid pressure below the water column

$\sigma_{v,0}$: vertical stress given by weight of the water column

(Modified after Johann et al., 2018)

Modelling - Time-Dependent Boundary Condition

Analytic Solution
Modified uniaxial loading problem: 1D
based on Shapiro (2015)

Numerical Model
FEM (COMSOL®): 2D plane strain

Modelling - Time-Dependent Boundary Condition

Analytic Solution

Modified uniaxial loading problem: 1D based on Shapiro (2015)

Numerical Model

FEM (COMSOL®): 2D plane strain

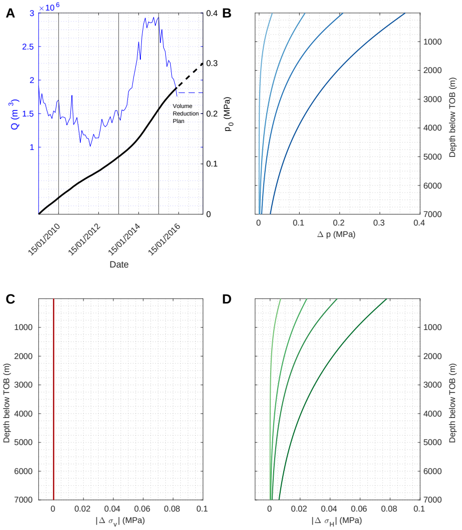

Synthetic Seismicity

Triggering criterion (Rothert and Shapiro, 2003):

$$\boxed{\Delta FCS(z,t) > C(z)}$$

$\Delta FCS(z,t) = 0.5\Delta\sigma_d - \sin\phi_f\,(\Delta\sigma_m - \Delta p)$: Change in failure criterion stress

$C(z)$: ΔFCS, necessary for activation of critically stressed, favorably oriented preexisting fractures

Synthetic Seismicity

Triggering criterion (Rothert and Shapiro, 2003):

$$\boxed{\Delta FCS(z,t) > C(z)}$$

$\Delta FCS(z,t) = 0.5\Delta\sigma_d - \sin\phi_f\,(\Delta\sigma_m - \Delta p)$: Change in failure criterion stress

$C(z)$: ΔFCS, necessary for activation of critically stressed, favorably oriented preexisting fractures

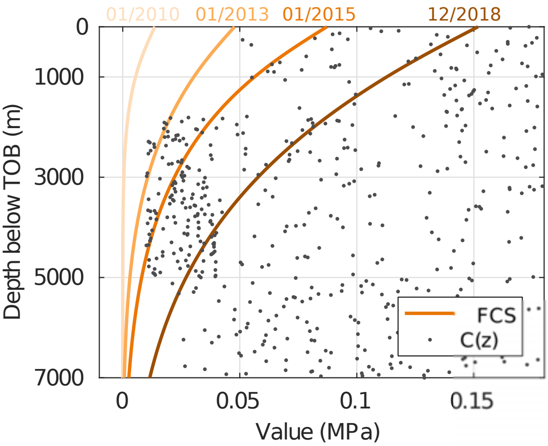

Here:

ΔFCS: for a strike-slip regime

C: log-normally distributed with layers of higher/ lower values in the upper/lower basement

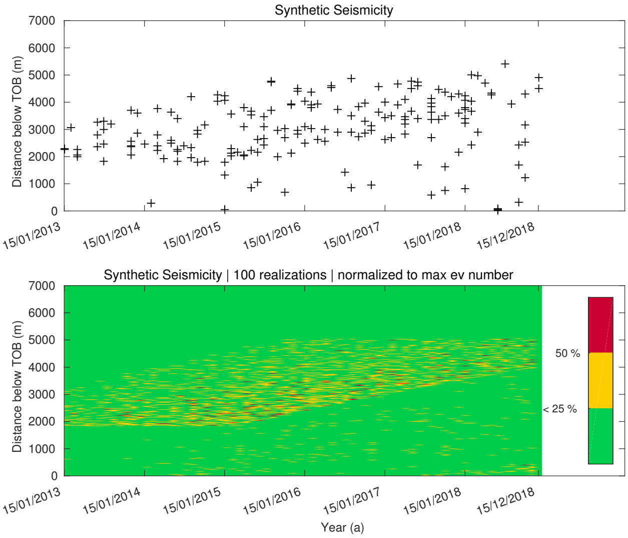

(From Johann et al., 2018)

Oklahoma Seismicity

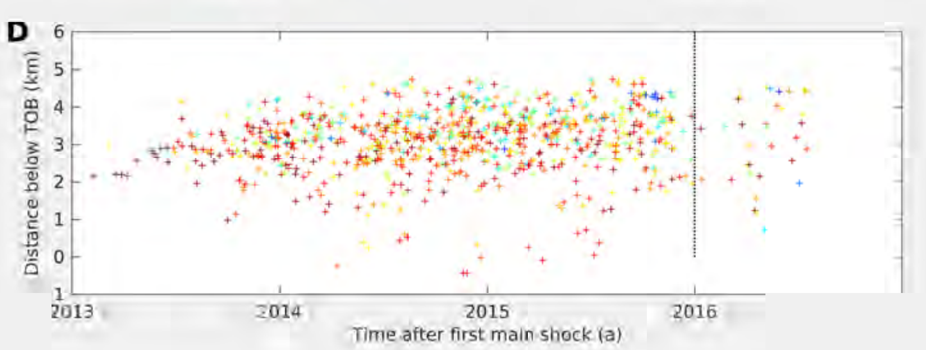

(Catalog from Schoenball and Ellsworth, 2017)

General conformity of spatio-temporal evolution in model years 3 ($\rightarrow$ 2013) to 5 ($\rightarrow$ 2016)

Seismicity Rates

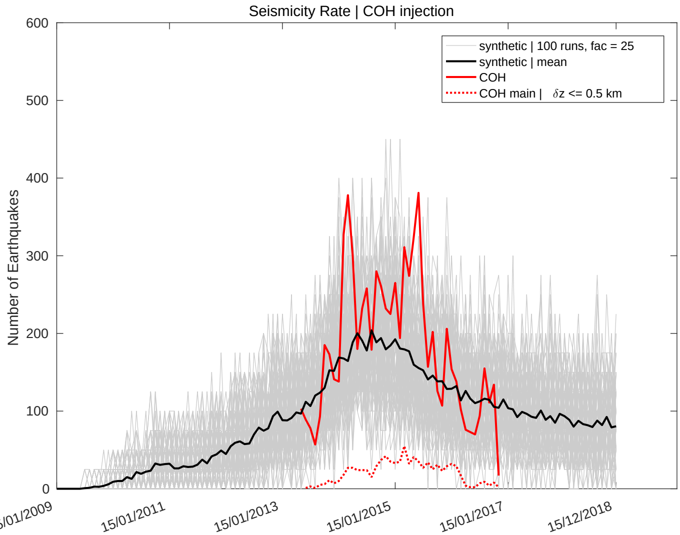

(From Johann et al., 2018)

URIS Model 2.0: Consider the effect of the water origin

So far...

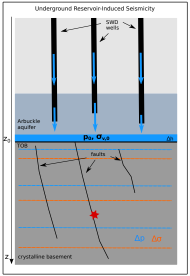

(Modified after Johann et al., 2018)

Now:

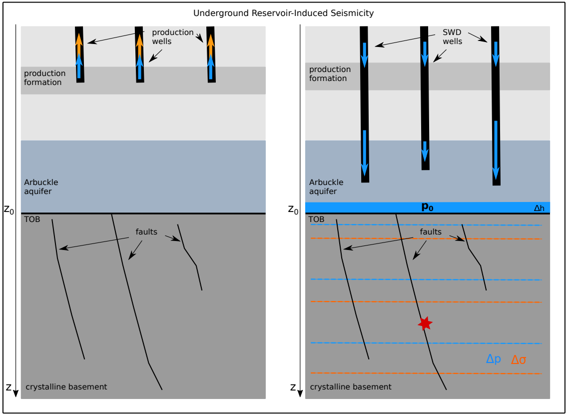

Note:

p_0: pore-fluid pressure below the water column

$\sigma_{v,0}$ is removed

Pressure- & Stress Solutions: Influence of the Tectonic Setting

Modified URIS

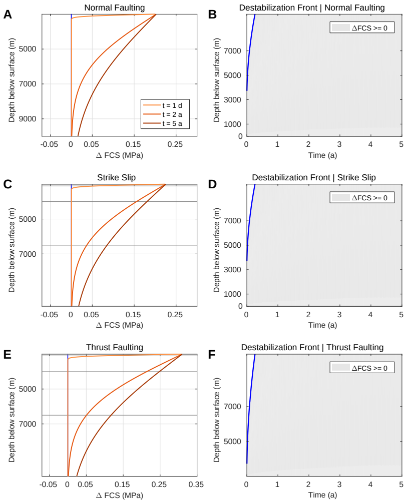

Pressure- & Stress Solutions: Influence of the Tectonic Setting

Modified URIS

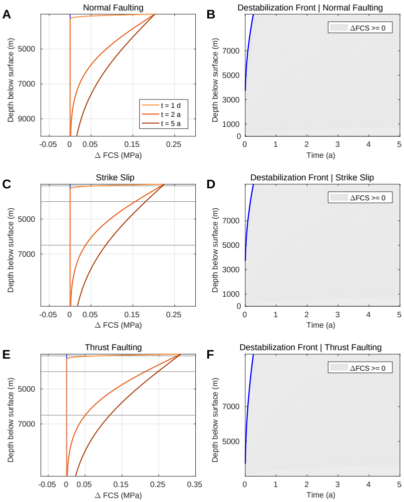

URIS

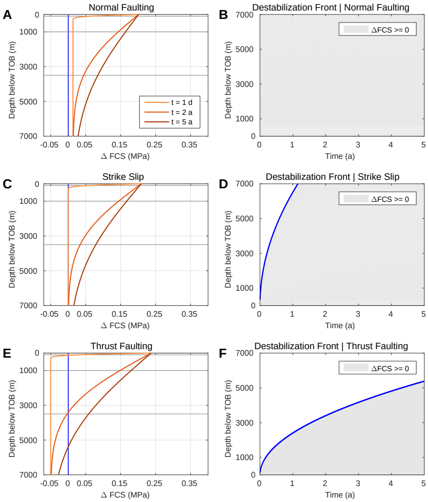

Time-Dependent Boundary: Synthetic Seismicity

Modified URIS

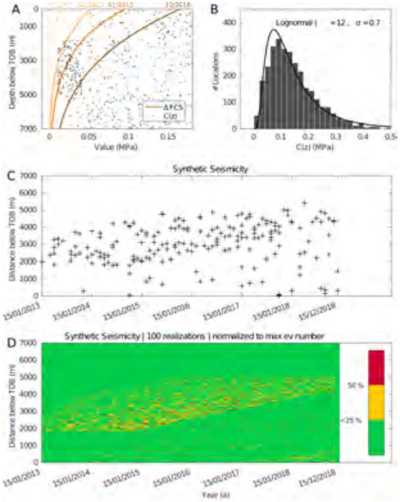

Time-Dependent Boundary: Synthetic Seismicity

Modified URIS **URIS**

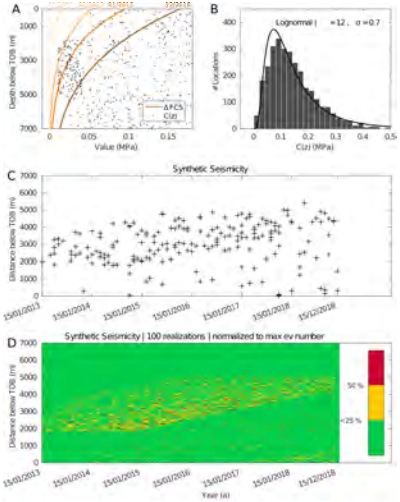

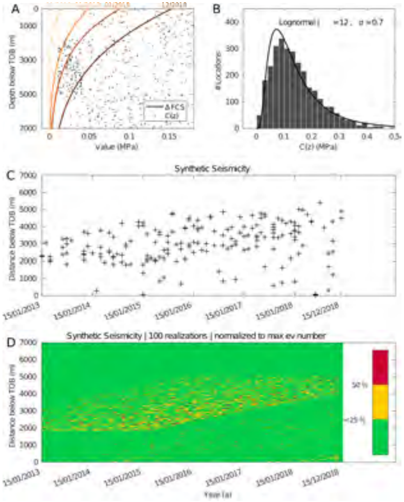

(From Johann et al., 2018)

Summary & Conclusions

- A new model for seismicity induced by high-volume fluid injections (e.g. waste water disposal)
- Based on Reservoir-Induced Seismicity, i.e. uniaxial loading of a poroelastic half-space
- Seismic activity is sensitive to the tectonic stress regime
- Spatio-temporal signatures of seismicity in Central Oklahoma (05/2013 - 11/2016) are well explained by the URIS model
- *Taking the origin of the waste water into account (i.e. no vertical stress acting on the TOB), does not change ΔFCS for a strike-slip regime significantly, but has an important effect regarding normal and thrust faulting regimes*

$\Rightarrow$ Provides an important contribution for the hazard assessment and seismic risk mitigation at waste water disposal sites.

Summary & Conclusions

- A new model for seismicity induced by high-volume fluid injections (e.g. waste water disposal)
- Based on Reservoir-Induced Seismicity, i.e. uniaxial loading of a poroelastic half-space
- Seismic activity is sensitive to the tectonic stress regime
- Spatio-temporal signatures of seismicity in Central Oklahoma (05/2013 - 11/2016) are well explained by the URIS model
- *Taking the origin of the waste water into account (i.e. no vertical stress acting on the TOB), does not change ΔFCS for a strike-slip regime significantly, but has an important effect regarding normal and thrust faulting regimes*

$\Rightarrow$ Provides an important contribution for the hazard assessment and seismic risk mitigation at waste water disposal sites.

Summary & Conclusions

- A new model for seismicity induced by high-volume fluid injections (e.g. waste water disposal)
- Based on Reservoir-Induced Seismicity, i.e. uniaxial loading of a poroelastic half-space
- Seismic activity is sensitive to the tectonic stress regime
- Spatio-temporal signatures of seismicity in Central Oklahoma (05/2013 - 11/2016) are well explained by the URIS model
- *Taking the origin of the waste water into account (i.e. no vertical stress acting on the TOB), does not change ΔFCS for a strike-slip regime significantly, but has an important effect regarding normal and thrust faulting regimes*

$\Rightarrow$ Provides an important contribution for the hazard assessment and seismic risk mitigation at waste water disposal sites.

Summary & Conclusions

- A new model for seismicity induced by high-volume fluid injections (e.g. waste water disposal)
- Based on Reservoir-Induced Seismicity, i.e. uniaxial loading of a poroelastic half-space
- Seismic activity is sensitive to the tectonic stress regime
- Spatio-temporal signatures of seismicity in Central Oklahoma (05/2013 - 11/2016) are well explained by the URIS model
- *Taking the origin of the waste water into account (i.e. no vertical stress acting on the TOB), does not change ΔFCS for a strike-slip regime significantly, but has an important effect regarding normal and thrust faulting regimes*

$\Rightarrow$ Provides an important contribution for the hazard assessment and seismic risk mitigation at waste water disposal sites.

Summary & Conclusions

- A new model for seismicity induced by high-volume fluid injections (e.g. waste water disposal)
- Based on Reservoir-Induced Seismicity, i.e. uniaxial loading of a poroelastic half-space
- Seismic activity is sensitive to the tectonic stress regime
- Spatio-temporal signatures of seismicity in Central Oklahoma (05/2013 - 11/2016) are well explained by the URIS model
- *Taking the origin of the waste water into account (i.e. no vertical stress acting on the TOB), does not change ΔFCS for a strike-slip regime significantly, but has an important effect regarding normal and thrust faulting regimes*

$\Rightarrow$ Provides an important contribution for the hazard assessment and seismic risk mitigation at waste water disposal sites.

Thank You!

We thank the sponsors of the *PHASE* consortium for supporting the research presented in this talk

References I

Chang, K. W. and Segall, P. (2016). Injection-induced seismicity on basement faults including poroelastic stressing. *Journal of Geophysical Research: Solid Earth*, 121:2708 – 2726.

Johann, L., Shapiro, S. A., and Dinske, C. (2018). The surge of earthquakes in Central Oklahoma has features of reservoir-induced seismicity. *Sci. Rep.*, 8.

Langenbruch, C., Weingarten, M., and Zoback, M. (2018). Physics-based forecasting of man-made earthquake hazards in Oklahoma and Kansas. *Nat. Commun.*, 9.

Norbeck, J. H. and Horne, R. N. (2016). Evidence for a transient hydromechanical and frictional faulting response during the 2011 Mw 5.6 Prague, Oklahoma earthquake sequence. *Journal of Geophysical Research: Solid Earth*, 121(12):8688–8705.

Rothert, E. and Shapiro, S. A. (2003). Microseismic monitoring of borehole fluid injections: Data modeling and inversion for hydraulic properties of rocks. *Geophysics*, 68:685–689.

Schoenball, M. and Ellsworth, W. (2017). Waveform-Relocated Earthquake Catalog for Oklahoma and Southern Kansas Illuminates the Regional Fault Network. *Seismol. Res. Lett.*, 88(4).

References II

Shapiro, S. (2015). *Fluid-Induced Seismicity*. Cambridge Univerisity Press, Cambridge, U.K.

Simpson, D. W., Leith, W. S., and Scholz, C. H. (1988). Two types of reservoir-induced seismicity. *Bull. Seismol. Soc. Am.*, 78(6):2025–2040.

Talwani, P. (1997). On the Nature of Reservoir-induced Seismicity. *Pure Appl. Geophys.*, 150:473–492.

Appendix

EQ Catalog

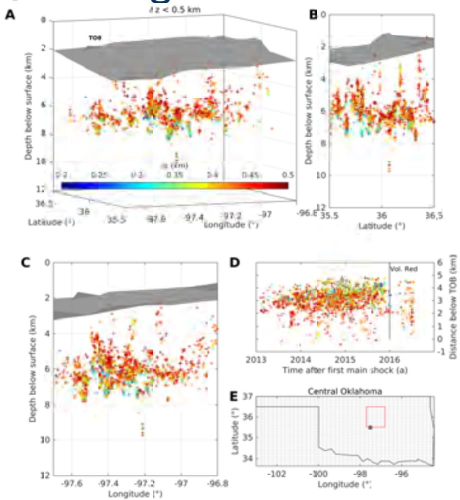
A
B
C
D
E
Depth below surface (km)
Latitude (°)
Longitude (°)
Vol. Red
Distance below TOB (km)
Time after first main shock (a)
Central Oklahoma

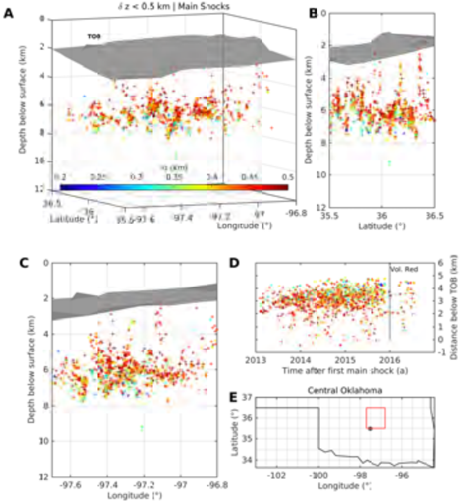
A
B
C
D
E
Depth below surface (km)
Latitude (°)
Longitude (°)
Vol. Red
Distance below TOB (km)
Time after first main shock (a)
Central Oklahoma

Declustering

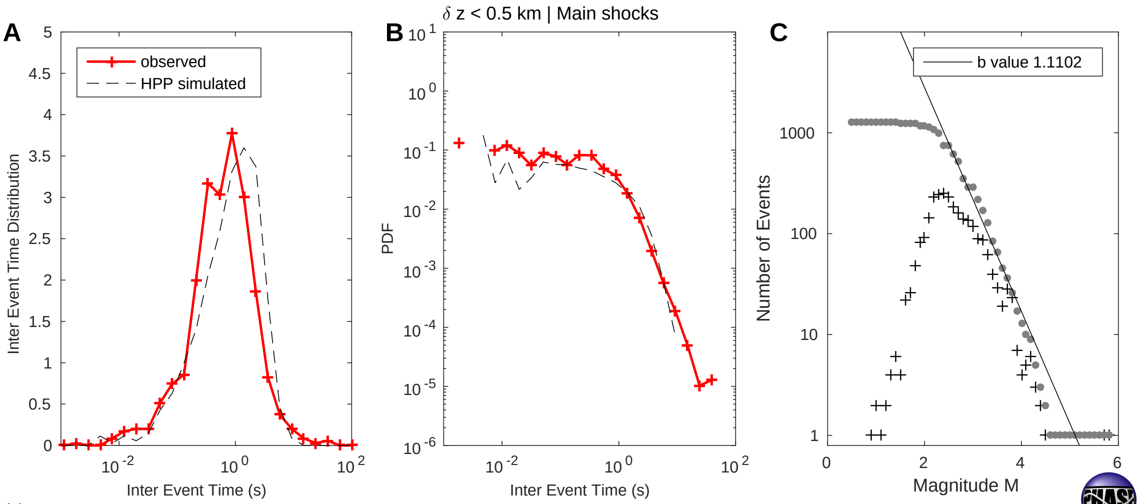

Analytic Solution

For a poroelastic medium & gravity acting in vertical z-direction (based on Shapiro, 2015), $\sigma < \mathbf{0}$**: compressive stress**:

$$p(z,t) = H_f + \rho_f g(z - z_0) + p_0 h(t)\left[\Phi_{Ar}\frac{n_S}{G_{dr}S} + \operatorname{erfc}\left(\frac{z - z_0}{\sqrt{4Dt}}\right)\left[1 - \Phi_{Ar}\frac{n_S}{G_{dr}S}\right]\right]$$

$$\sigma_{zz}(z,t) = -H_s - \rho g(z - z_0) - h(t)p_0\Phi_{Ar}$$

$$\sigma_{xx}(z,t) = \sigma_{yy}(z,t) = \lambda_{dr}\epsilon_{zz}(z,t) - \alpha p(z,t)$$

z_0: top of the basement
H_f, H_s: hydrostatic pressure and lithostatic stress at z_0 (const.)
ρ, ρ_f: matrix and pore fluid density
G_{dr}, λ_{dr}, α: drained shear, first Lamé parameter and the Biot coefficient
$n_S = \frac{\alpha G_{dr}}{\lambda_{dr} + 2G_{dr}}$: poroelastic stress coefficient
S, D: storage coefficient and the hydraulic diffusivity
p_0: boundary pressure / stress

Numerical Model

Finite element model performed with COMSOL Multiphysics software: 2D plane strain

Hydro-mechanical parameters

Hydraulic diffusivity D	0.05 (m^2/s)
Porosity Φ	1 (%)
Drained density ρ_{dr}	2740 (kg/m^3)**
First Lamé parameter λ_{dr}	20 (GPa)
Second Lamé parameter G_{dr}	25 (GPa)**
Fluid density ρ_f	940.3 (kg/m^3)*
Dynamic viscosity η	2e-04 (Pas)*
Bulk modulus fluid K_f	2 (GPa)*
Biot coefficient α	0.3
Coefficient of friction μ_f	0.7
Porosity Arbuckle Φ_{Ar}	20 (%)

*Norbeck and Horne (2016), **Chang and Segall (2016)

Modelling

Analytic Solution
Modified uniaxial loading problem: 1D based on Shapiro (2015)

Numerical Model
FEM (COMSOL®): 2D plane strain

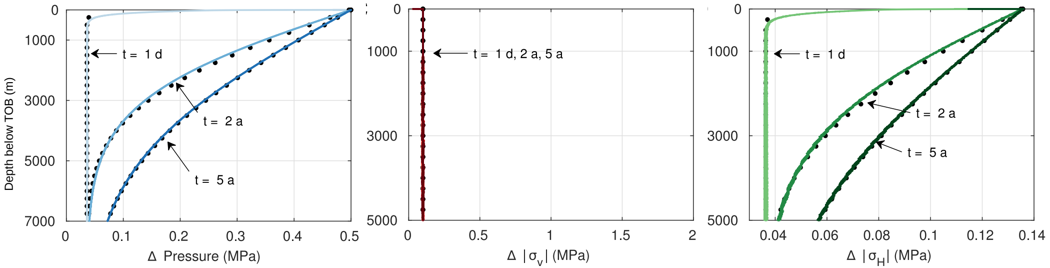

Failure Criterion Stress for optimally oriented faults

$$\Delta FCS = \frac{1}{2}\Delta\sigma_d - \sin\phi_f\left(\Delta\sigma_m - \Delta p\right)$$

$\Delta FCS > 0$: Destabilization
$\Delta FCS < 0$: Stabilization

Sensitivity Study

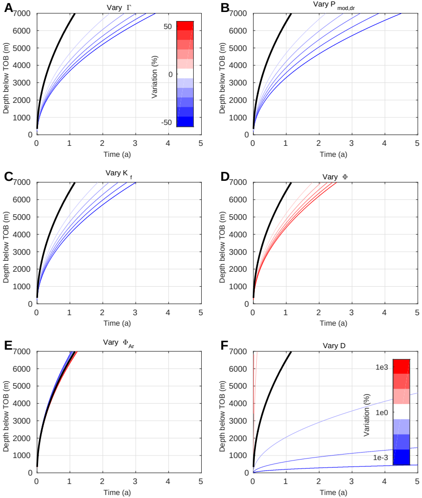

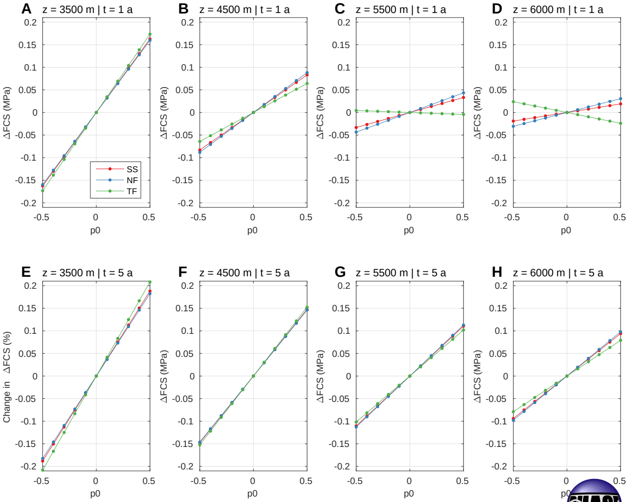

Synthetic $r-t$-plot: Uncertainty

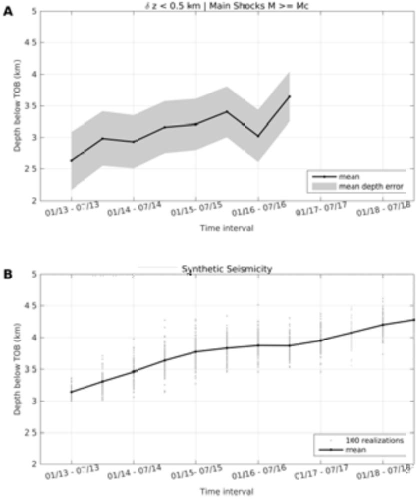

Modified URIS: Analytic Solution

For a poroelastic medium & gravity acting in vertical z-direction
(based on Shapiro, 2015; Johann et al., 2018), $\sigma < \mathbf{0}$**: compressive stress**:

$$\Delta p(z,t) = p_0 h(t) \mathrm{erfc}\left(\frac{z - z_0}{\sqrt{4Dt}}\right),$$

$$\Delta\sigma_{zz}(z,t) = 0\,,$$

$$\Delta\epsilon_{zz}(z,t) = \frac{\alpha p(z,t)}{\lambda_{dr} + 2G_{dr}}\,,$$

$$\Delta\sigma_{xx}(z,t) = \sigma_{yy}(z,t) = \lambda_{dr}\epsilon_{zz}(z,t) - \alpha p(z,t)\,.$$

z_0: top of the basement
ρ, ρ_f: matrix and pore fluid density
G_{dr}, λ_{dr}, α: drained shear, first Lamé parameter and the Biot coefficient
$n_S = \frac{\alpha G_{dr}}{\lambda_{dr}+2G_{dr}}$: poroelastic stress coefficient
S, D: storage coefficient and the hydraulic diffusivity
p_0, s_0: boundary pressure / stress

Modified URIS: ΔFCS Contributions